

# New geochemical data on fossil wood from the Albian of the Dolomites (Southern Alps, Italy)

ALEXANDER LUKENEDER<sup>1</sup>, ACHIM BECHTEL<sup>2</sup> and REINHARD GRATZER<sup>2</sup>

<sup>1</sup>Natural History Museum, Geological-Paleontological Department, Burgring 7, 1010 Wien, Austria; alexander.lukeneder@nhm-wien.ac.at

<sup>2</sup>Department of Applied Geosciences and Geophysics, University of Leoben, Peter-Tunner-Str. 5, A-8700 Leoben, Austria; achim.bechtel@unileoben.ac.at; reinhard.gratzer@unileoben.ac.at

(Manuscript received November 15, 2011; accepted in revised form March 13, 2012)

**Abstract:** Information is provided about organic-matter bearing sediments and fossil drift-wood from the Puez area (Col de Puez, Southern Alps) near Wolkenstein (S. Tyrol, Italy). The locality is located on the Trento Plateau which represents a submarine high during the Lower Cretaceous. Its terpenoid hydrocarbon composition indicates that the wood fragment derived from a conifer belonging to the family Podocarpaceae or Araucariaceae. Intense degradation of OM argues for lengthier drifting. Long-term drifting is also indicated by the infestation of the bivalve *Teredo* (“ship-worm”). The finding of a fossil tree trunk sheds some light on the early Lower Cretaceous tectonic history of the Trento Plateau and the Dolomites.

**Key words:** Drift-wood, Albian, Early Cretaceous, Dolomites, Italy.

## Introduction

The geology of the Dolomites and adjacent areas has recently been summarized in detail by Lukeneder & Aspmair (2006), and Lukeneder (2008, 2010, 2011). According to recent investigations by Muttoni et al. (2005), the Lombardian Basin — and thus the adjacent Trento Plateau to the east — were located at approximately 35 °N to 25 °N in the Early Jurassic, at 10 °N in the Middle-Late Jurassic (lowest latitude in the Kimmeridgian), at approximately 20 °N in the Valanginian-Hauterivian time and back to almost 30 °N in the Early Cretaceous (Aptian).

The complex Mediterranean paleogeography of Jurassic and Cretaceous domains (Fourcade et al. 1993) is characterized by microplates within the Tethyan oceanic corridor between the African and European landmasses (Dercourt et al. 1993; Cecca 1998; Zharkov et al. 1998; Stampfli & Mosar 1999; Scotese 2001; Stampfli et al. 2002). The region of the Southern Alps, including the investigated area (i.e. Puez area), was situated on the northern border to the Penninic Ocean (= Alpine Tethys) during the Jurassic and Early Cretaceous. This area represents a passive continental margin of the Apulian Plate (Jud 1994) of the South Alpine-Apennine Block. It was delimited by the Penninic Ocean to the north-west and the Vardar Ocean to the south-east (Dercourt et al. 1993; Stampfli & Mosar 1999; Scotese 2001; Stampfli et al. 2002).

The stratigraphy of the Lower Cretaceous sediments here is based on micro- and nannofossils (e.g. foraminifera, calpionellids and dinoflagellates; see also Lukeneder 2010) and macrofossils (ammonites; Lukeneder 2012).

The main goal is to present new geochemical data on Lower Cretaceous fossil wood from the Dolomites. The presented data provide the first insights into Albian fossil wood from the Dolomites and were collected within the Dolomite Project P20018-N10 (Project of the Austrian Science Fund FWF).

## Geographical and geological setting

### Geography

The outcrop is situated on the Puez-Odle-Gardenaccia Plateau in the Dolomites, 30 km northeast of Bozen, 6 km northeast of Wolkenstein (= Selva in Val Gardena, = Sölva), in the Department Trentino-Alto Adige (maps Trentino — Alto Adige; South Tyrol, Italy; Tappeiner 2003). The locality is situated in the heart of the natural park Puez-Odle within the UNESCO world heritage area of the Dolomites (Lukeneder 2010, 2011, 2012; Fig. 1).

### Geological setting

The Puez area is situated on the northernmost part of the Trento Plateau within the Dolomites, formed on a Cretaceous submarine plateau, the Puez-Gardenaccia Plateau. The Dolomites (Permian to Cretaceous) are an internal part of the Southern Alps, representing a Northern Italian mountain chain that emerged during the deformation of the passive continental margin of the Adriatic (Jud 1994; Bosellini et al. 2003; Castellarin et al. 2006). For a more detailed geology of the Puez area see Lukeneder (2010, 2011, 2012).

The Albian Puez-Marl Member (approximately 60 m, Early Albian-Early Cenomanian) encompasses the marl-rich upper part of the Puez Formation (for a discussion see Lukeneder & Aspmair 2006; Lukeneder 2008, 2010, 2012). The analysed tree trunk derives from the mid part of this member, section Puez/P2 (bed P2/160; Figs. 1–2).

Biostratigraphical data (Lukeneder 2010; pers. comm. J. Soták) indicate *Hedbergella* ssp. and *Rotalipora* ssp. (up to the *Thalmaninella globotruncanoides* Biozone) along with calcareous nannofossils such as *Eiffellithus* ssp. (up to latest Albian CC9 Zone) and hint at an Early Albian to Late Albian

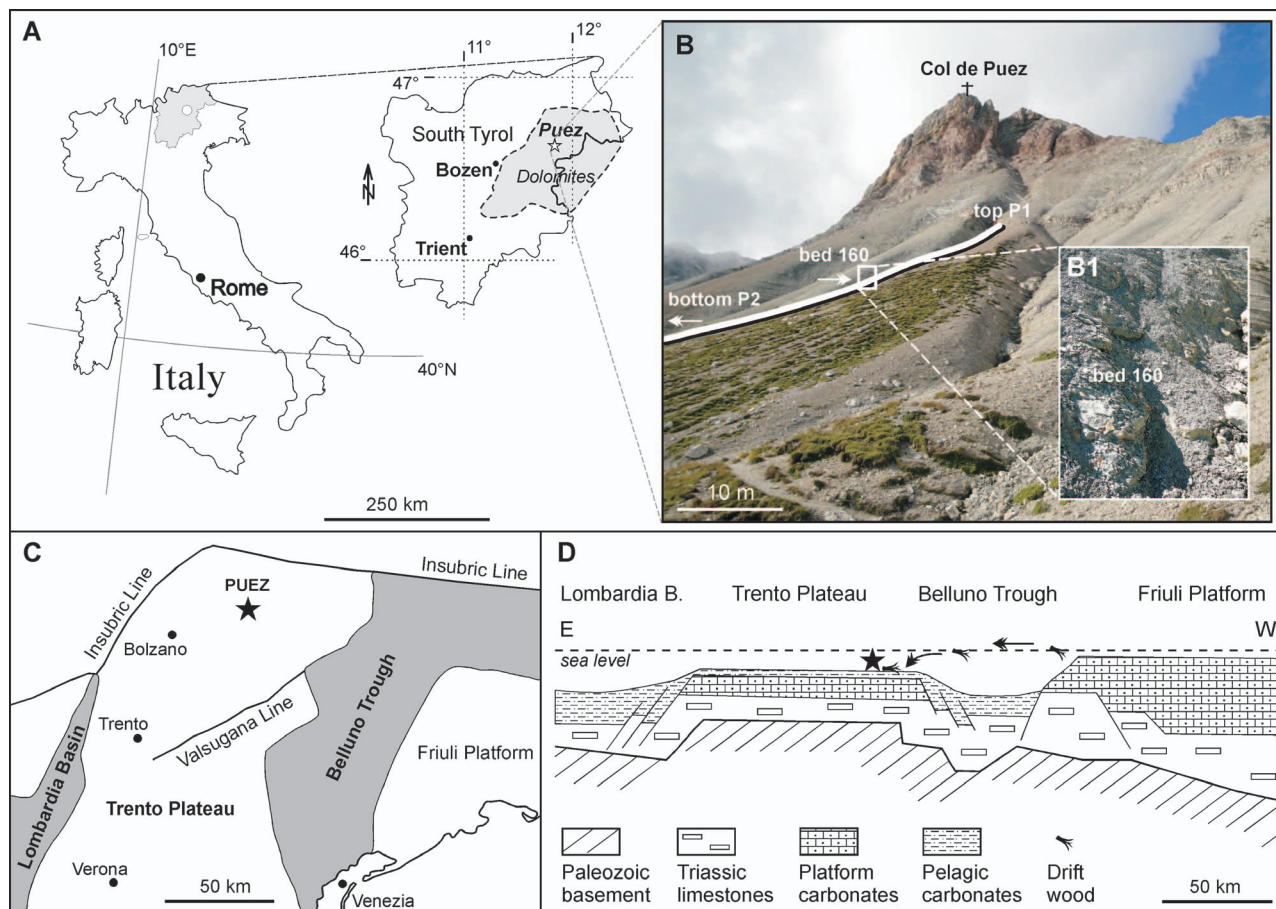


**Fig. 1.** Locality map of the Puez area with indicated outcrop position of the main log Puez P2 within the Dolomites (S. Tyrol, Italy). **A** — Puez area (white star) and indicated outcrop position (P1). **B** — Detailed position of the drift-wood bed P2 160 at the Col de Puez section. **B1** — Enlarged part of the dark, marl-bed P2 160. **C** — Position of the Puez Locality on the Trento Plateau. **D** — East-west transect during the Lower Cretaceous plateau-basinal sequence of the South Alpine region, (not palinsparically corrected), modified after Caracuel et al. (1997) and Pr at et al. (2006). Note indicated drift wood. Adapted after Lukeneder (2011, 2012).

age (perhaps up to the Albian/Cenomanian boundary) for the Puez-Marl Member. The drift wood bed P2/160 shows Mid Albian age.

### Material and methods

Drifted wood is not known from the Lower Cretaceous of the Southern Alpine region so far. The tree trunk (approximately 15×20 cm) derives from the mid part of the section Puez/P2 (log P2/160; Figs. 1–2). The specimen is covered by a yellowish layer consisting of limonite (Fig. 2). The still attached surrounding sediment comprised radiolarians and foraminifera. The trunk is well preserved and each wood fibre and cell is visible in detail. The specimen shows a trunk with the branching of a limb.

Beds were sampled for biostratigraphical (macro- and microfossils), and geochemical (CaCO<sub>3</sub>) data. Calcium carbonate contents (CaCO<sub>3</sub>; wt. % bulk rock, total carbonate) were determined using the carbonate bomb technique. All the chemical analyses were carried out in the laboratories of the Department of Applied Geosciences and Geophysics, Mon-

tanuniversit t Leoben. Samples are stored at the Natural History Museum of Vienna (NHMW), in the collection of the Department of Geology and Palaeontology with inventory number from NHMW 2010/0095/0001. Microfossil analysis includes preliminary studies of foraminifera by J n Sot k.

### Organical geochemistry

For organic geochemical analyses, representative portions of selected samples were extracted for approximately 1 h using dichloromethane in a Dionex ASE 200 accelerated solvent extractor at 75 °C and 50 bar. After evaporation of the solvent to 0.5 ml total solution in a Zymark TurboVap 500 closed cell concentrator, asphaltenes were precipitated from a hexane-dichloromethane solution (80:1) and separated by centrifugation. The fractions of the hexane-soluble organic matter were separated into NSO compounds, saturated hydrocarbons, and aromatic hydrocarbons by medium-pressure liquid chromatography using a K hnen-Willsch MPLC instrument (Radke et al. 1980).

The saturated and aromatic hydrocarbon fractions were analysed on a gas chromatograph equipped with a 30-m DB-1

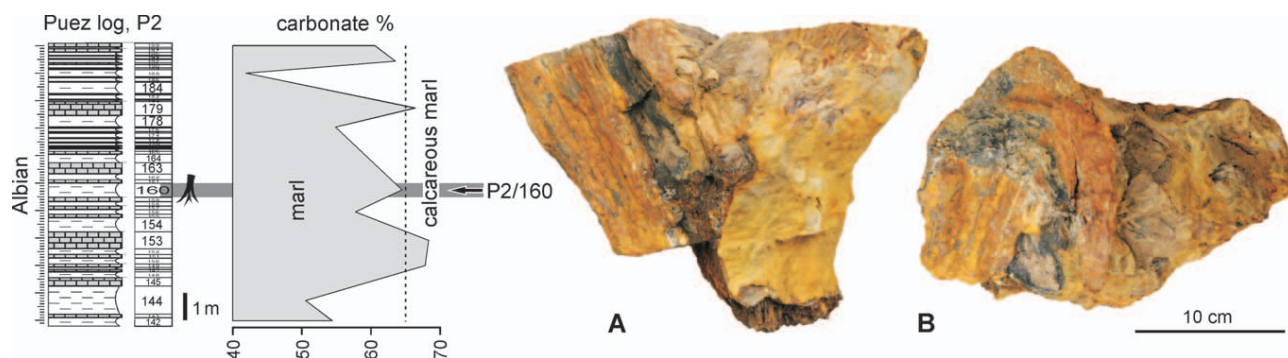


**Fig. 2.** Lithostratigraphic column with plotted carbonate content around the drift-wood bed P2/160. Note the indicated grey-bold line which marks the position of bed P2/160, the drift-wood bed. **A** — Frontal view of the drift wood showing limonitic preservation on surface. **B** — Top view of the same specimen.

fused silica capillary column (i.d. 0.25 mm; 0.25-mm film thickness) and coupled to a Finnigan MAT GCQ ion trap mass spectrometer. The oven temperature was programmed from 70° to 300 °C at a rate of 4 °C·min<sup>-1</sup> followed by an isothermal period of 15 min. Helium was used as carrier gas. The sample was injected splitless with the injector temperature at 275 °C. The mass spectrometer was operated in the EI (electron impact) mode over a scan range from *m/z* 50 to *m/z* 650 (0.7 s total scan time). Data were processed with a Finnigan data system. Individual compounds were identified based on retention time in the total ion current (TIC) chromatogram and then comparing the mass spectra with published data. Relative percentages and absolute concentrations of different compound groups in the saturated and aromatic hydrocarbon fractions were calculated using peak areas from the gas chromatograms in relation to those of internal standards (deuterated *n*-tetracosane and 1.1'-binaphthyl, respectively). The concentrations were normalized to the total organic carbon content.

## Results and discussion

### Molecular composition of hydrocarbons

#### *n*-Alkanes, isoprenoids

The *n*-alkane patterns of most samples are dominated by short-chain *n*-alkanes (>*n*-C<sub>15-19</sub>). The short-chain *n*-alkanes (<C<sub>20</sub>), which are predominantly found in algae and microorganisms (Cranwell 1977), are detected in high relative amounts (>30 % of the total *n*-alkane concentrations) in the sediment samples (Table 2; Fig. 5). The predominance of *n*-alkanes with even carbon numbers (e.g. *n*-C<sub>14</sub>, *n*-C<sub>16</sub>, *n*-C<sub>18</sub>) indicates reducing conditions during early diagenesis of the sediments (Welte & Waples 1973). In contrast, long-chain *n*-alkanes (>*n*-C<sub>23</sub>) are characterized by a slight odd over even

predominance, as indicated by values of the Carbon Preference Index (CPI) between 1.2 and 1.4 (Table 2; Fig. 3). The CPI was calculated from the concentrations of individual *n*-alkanes using the formula of Bray & Evans (1961). Long-chain (C<sub>27</sub>-C<sub>31</sub>) *n*-alkanes are interpreted to be derived from vascular plants, where they occur as the main components of plant waxes (Eglinton & Hamilton 1967). Clearly, land plant organic matter had experienced aerobic degradation before its deposition in the sedimentary environment.

The fossil wood sample is characterized by the complete absence of short-chain *n*-alkanes and no odd over even predominance in the long-chain homologues (Table 2; Fig. 3). The CPI close to 1.0 and the presence of a hump in the high-molecular range argues for intense biodegradation of the fossil wood.

According to Didyk et al. (1978), pristane/phytane ratios between 1.0 and 3.0 indicate dysaerobic conditions during early diagenesis. This is in contrast to the reducing environment indicated by the even carbon number predominance of short-chain *n*-alkanes. However, pristane/phytane ratios are also known to be affected by maturation (Tissot & Welte 1984) and by differences in the precursors for acyclic isoprenoids (i.e. bacterial origin; Volkman & Maxwell 1986; ten Haven et al. 1987). In the present case, the influence of different ranks on pristane/phytane ratios can be ruled out.

**Table 1:** Bulk organic geochemical data of sediment samples and fossil wood.

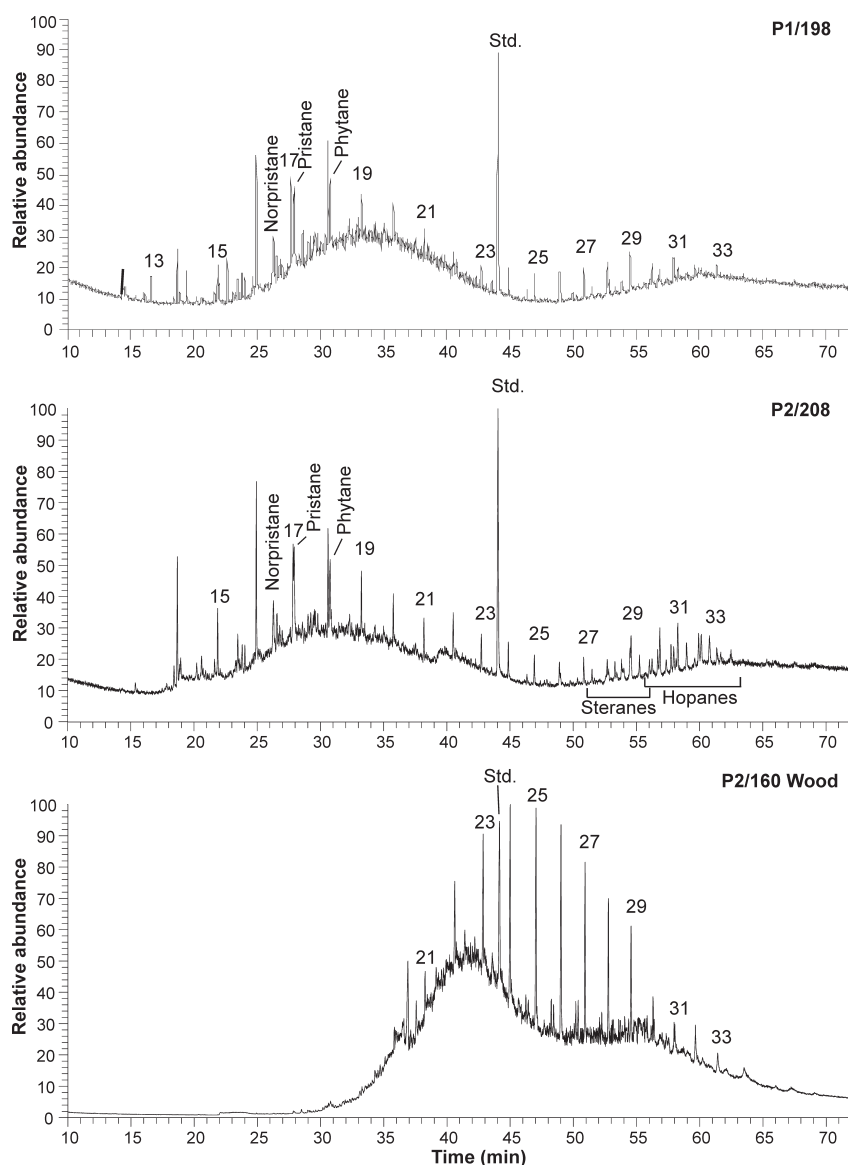
| Sample           | TOC          | EOM         | Saturated HC | Aromatic HC  | NSO          | Asphaltenes  |
|------------------|--------------|-------------|--------------|--------------|--------------|--------------|
|                  | (wt. %)      | (mg/g TOC)  | (wt. %, EOM) | (wt. %, EOM) | (wt. %, EOM) | (wt. %, EOM) |
| P1/18            | 0.20         | 21.8        | 20           | 11           | 56           | 13           |
| P1/71b           | 0.25         | 23.1        | 21           | 2            | 63           | 14           |
| P1/198           | 0.20         | 31.6        | 16           | 6            | 64           | 14           |
| P2/35            | 0.39         | 10.7        | 13           | 4            | 66           | 17           |
| P2/96            | 0.48         | 14.0        | 16           | 4            | 71           | 9            |
| P2/104           | 0.31         | 19.8        | 10           | 2            | 67           | 21           |
| P2/138           | 0.49         | 11.2        | 15           | 5            | 76           | 4            |
| P2/208           | 0.38         | 19.5        | 15           | 3            | 78           | 5            |
| P2/247           | 0.74         | 6.1         | 12           | 2            | 81           | 5            |
| P2/268a          | 0.69         | 8.4         | 15           | 3            | 77           | 5            |
| P3/1a            | 0.25         | 17.2        | 18           | 2            | 73           | 7            |
| P3/19            | 0.22         | 33.8        | 13           | 5            | 77           | 6            |
| <b>P2/160 FW</b> | <b>14.25</b> | <b>65.7</b> | <b>51</b>    | <b>2</b>     | <b>28</b>    | <b>19</b>    |

TOC = Total organic carbon, EOM = Extractable organic matter, HC = Hydrocarbons, NSO = NSO compounds.

**Table 2:** Concentration and concentration ratios of compounds and compound groups identified in the hydrocarbon fractions of the Puez samples.

| <i>n</i> -Alkanes<br>( $\mu\text{g/g TOC}$ ) | <i>n</i> -C <sub>15-19</sub> /<br><i>n</i> -Alkanes | <i>n</i> -C <sub>27-31</sub> /<br><i>n</i> -Alkanes | CPI  | Pristane/<br>Phytane | C <sub>27</sub><br>Steranes<br>( $\mu\text{g/g TOC}$ ) | C <sub>28</sub><br>Steranes<br>( $\mu\text{g/g TOC}$ ) | C <sub>29</sub><br>Steranes<br>( $\mu\text{g/g TOC}$ ) | Hopanes<br>( $\mu\text{g/g TOC}$ ) | Sesquiterpenoids<br>(Arom.)<br>( $\mu\text{g/g TOC}$ ) | Diterpenoids<br>(Arom.)<br>( $\mu\text{g/g TOC}$ ) | PAH<br>( $\mu\text{g/g TOC}$ ) |
|--|---|---|------|----------------------|--|--|--|------------------------------------|--|--|--------------------------------|
| 102  | 0.27  | 0.32  | 1.29 | 1.09                 | 1.4  | 1.1  | 1.7  | 25.2                               | 17.3   | 18.3   | 13.4                           |
| 282  | 0.44  | 0.24  | 1.30 | 0.96                 | 8.9  | 7.5  | 9.4  | 56.7                               | 13.2   | 14.0   | 10.2                           |
| 124  | 0.44  | 0.24  | 1.28 | 1.02                 | 1.8  | 1.5  | 2.1  | 23.1                               | 45.4   | 16.1   | 49.7                           |
| 51   | 0.45  | 0.17  | 1.18 | 0.91                 | 0.6  | 0.5  | 0.7  | 8.3                                | 32.9   | 2.5  | 4.8                            |
| 108  | 0.43  | 0.20  | 1.36 | 0.84                 | 4.8  | 3.0  | 6.1  | 30.8                               | 34.1   | 2.3  | 8.3                            |
| 55   | 0.52  | 0.16  | 1.43 | 1.10                 | 1.0  | 0.8  | 1.4  | 7.3                                | 34.3   | 2.4  | 11.9                           |
| 64   | 0.52  | 0.13  | 1.18 | 1.11                 | 1.3  | 1.2  | 1.6  | 7.7                                | 20.5   | 1.5  | 7.3                            |
| 66   | 0.51  | 0.15  | 1.41 | 1.15                 | 2.8  | 2.3  | 3.3  | 19.8                               | 24.9   | 3.7  | 13.4                           |
| 42   | 0.47  | 0.14  | 1.23 | 1.05                 | 0.6  | 0.5  | 0.7  | 4.7                                | 8.7  | 2.3  | 6.5                            |
| 40   | 0.50  | 0.12  | 1.32 | 0.93                 | 0.4  | 0.4  | 0.5  | 3.1                                | 10.3   | 2.5  | 5.2                            |
| 62   | 0.38  | 0.23  | 1.42 | 0.73                 | 1.1  | 1.0  | 1.6  | 9.3                                | 9.3  | 2.2  | 4.9                            |
| 117  | 0.50  | 0.13  | 1.34 | 1.38                 | 1.5  | 1.2  | 1.8  | 17.2                               | 34.9   | 6.9  | 13.3                           |
| 1970   | 0.00  | 0.32  | 1.04 |                      | 0.0  | 0.0  | 0.0  | 0.0                                | 11.3   | 2.4  | 11.4                           |

CPI = Carbon preference index, PAH = Polycyclic aromatic hydrocarbons.

**Fig. 3.** Gas chromatograms (total ion current) of saturated hydrocarbon fractions of two sediment samples (a, b), and the fossil wood (c). *n*-Alkanes are labelled according to carbon number. Std. = standard (deuterated *n*-tetracosane).

In contrast, a proportion of pristane may be derived from tocopherols (Goossens et al. 1984), or may simply reflect the contribution of land plants to organic matter accumulation (Tissot & Welte 1984). No acyclic isoprenoids of low-molecular weight are present in the saturated hydrocarbon fraction of the fossil wood sample, most probably due to intense biodegradation.

#### Steroids

In all sediment samples, the 5 $\alpha$  C<sub>27</sub> and C<sub>29</sub> steranes, dominating over the corresponding 5 $\beta$  steranes, are present in concentrations sufficient for peak integration (Table 2; Fig. 3). The C<sub>28</sub> pseudohomologues occur in lower relative concentrations. The presence of 5 $\beta$  steranes is in agreement with the immature character of the samples.

Algae are the predominant primary producers of C<sub>27</sub> sterols, while C<sub>29</sub> sterols are more typically associated with land plants (Volkman 1986). Nonetheless, numerous results from recent biomarker studies add to the growing list of microalgae that contain high proportions of 24-ethylcholesterol (Volkman et al. 1999). The occurrence of C<sub>27</sub> and C<sub>29</sub> steranes in the sediments is consistent with a mixed origin of organic matter from phytoplankton and land plants. In the EOM from the fossil wood, no steranes were detected.

#### Hopanoids

Hopanes are constituents of the non-aromatic cyclic triterpenoids in most

samples (Fig. 3; Table 2). The samples show similar patterns, characterized by the occurrence of  $17\alpha$ ,  $21\beta$ (H)-type hopanes from  $C_{27}$  to  $C_{32}$ , with  $C_{28}$  hopanes absent. The  $17\beta$ ,  $21\alpha$ (H) hopanes from  $C_{29}$  to  $C_{31}$  are present in very low amounts. The predominant hopanoid is either the  $\alpha\beta$ - $C_{30}$  hopane or the  $\alpha\beta$ - $C_{29}$  hopane. The most probable biological precursors of the hopanes are bacetrio-hopanepolyols (Ourisson et al. 1979; Rohmer et al. 1992). These compounds have been identified in aerobic bacteria and fungi, as well as in cryptogams (e.g. ferns, moss) and, most recently, sulphate-reducing bacteria (Blumenberg et al. 2006).

The ratio of the 22S/(22S+22R) isomers of the  $17\alpha$ ,  $21\beta$ (H)  $C_{31}$  hopanes of most samples is in the range of 0.51 to 0.55, close to the equilibrium value of ca. 0.6 (Mackenzie et al. 1982). These values argue for a thermal maturity equivalent to vitrinite reflectance values around 0.5 %  $R_r$  (Mackenzie & Maxwell 1981), slightly higher than the value of 0.4 %  $R_r$  measured within the fossil wood sample.

#### Sesquiterpenoids and diterpenoids

In all samples, sesquiterpenoid tetrahydrocadalene predominates in the aromatic hydrocarbon fractions (Fig. 4; Table 2). Further constituents of the aromatic sesquiterpenoids are calamenene, curcumene and cadalene (Simoneit & Mazurek 1982). The aromatic diterpenoids present in the samples consist of compounds of the abietane-type (e.g. simonellite, retene; Philip 1985) (Fig. 4; Table 2).

The sesqui- and diterpenoids are most probably derived from precursor molecules abundant in resins of conifers belonging to the families Podocarpaceae, Araucariaceae, and Cupressaceae (Noble et al. 1985; Otto & Wilde 2001). Araucariaceae and Podocarpaceae evolved during the Early Triassic and are therefore considered as the most probable precursor plants for the sesqui- and diterpenoids found in the EOM of the samples (Stewart 1983). In the fossil wood, only aromatic sesquiterpenoids were identified.

#### Polycyclic aromatic hydrocarbons

The polycyclic aromatic hydrocarbon (PAH) phenanthrene was detected in all samples (Fig. 4; Table 2). Phenanthrene and its methylated analogues derive from a variety of non-specific precursor compounds such as steroids and triterpenoids (Tissot & Welte 1984). Polycyclic aromatic hydrocarbons (PAHs) with 4–5 rings ranging from fluoranthene to benz-(ghi)-perylene are present in the samples (Fig. 4). In recent sediments, combustion products

of fossil fuels represent the main source of these PAHs (Laflamme & Hites 1978). PAHs in ancient sediments may result from wildfires (Killops & Killops 1993), or may be formed during microbially mediated diagenetic processes (Alexander et al. 1992). Some compounds (i.e. perylene) may derive from polyaromatic precursors synthesized by living organisms such as fungi (Tissot & Welte 1984).

The PAHs present in the samples and the absence of their methylated analogues argue for the origin of these compounds from charcoal and/or an input of PAHs attributed to recurring forest or swamp fires. However, as outcrop samples are being investigated here, an anthropogenic source (i.e. combustion products of fossil fuels) cannot be excluded. Furthermore, perylene is the dominating compound in most samples. For this PAH, a variety of biological sources have been considered.

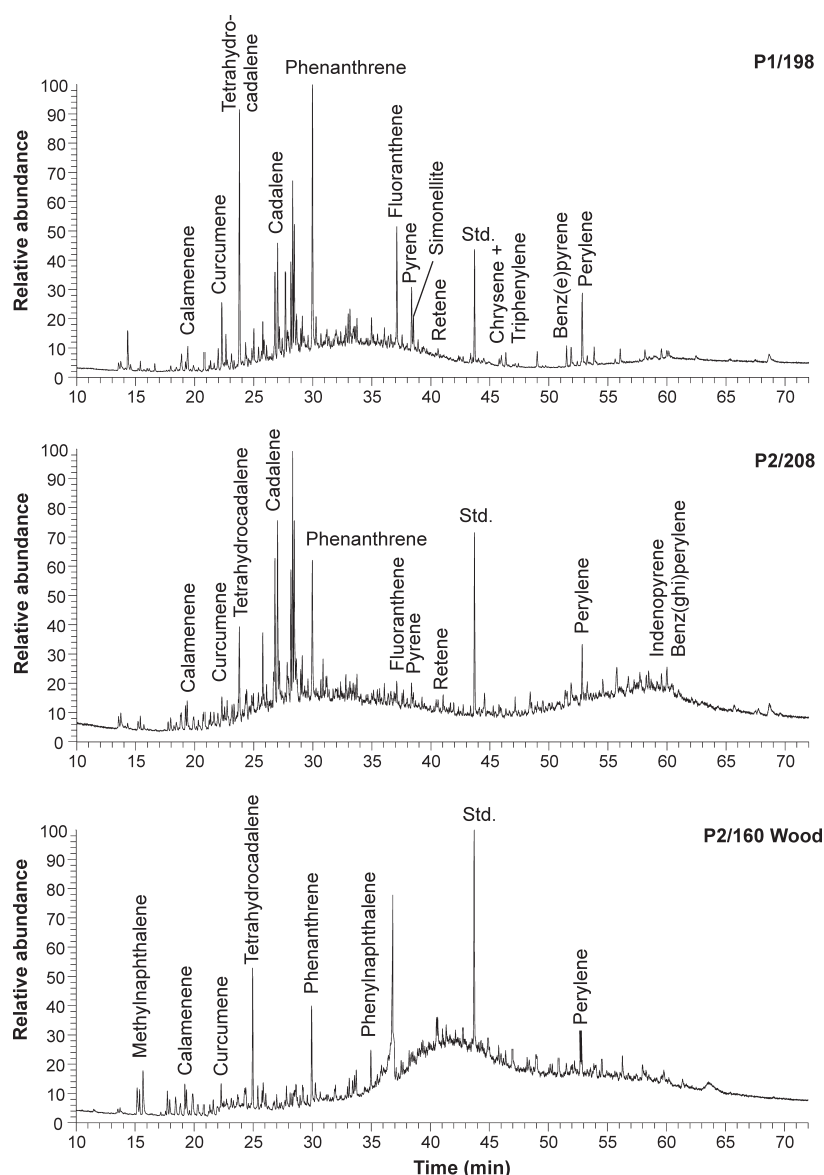


Fig. 4. Gas chromatograms (total ion current) of aromatic hydrocarbon fractions of two sediment samples (a, b), and the fossil wood (c). Std. = standard (1.1'-binaphthyl).

## Conclusions

Drift-wood is reported for the first time from the Lower Cretaceous of the Southern Alpine region. According to its terpenoid hydrocarbon composition, the wood fragment derived from a conifer belonging to the family Podocarpaceae or Araucariaceae. The age of the drift-wood is assigned to the Mid-Albian on the basis of the foraminifera fauna. The wood derives from surrounding islands formed during the beginning of the Alpine orogeny. The fossil wood was deposited after considerable drifting onto the sea-floor of the Albian Trento Plateau. Long-term drifting is indicated by the infestation of the bivalve *Teredo* ("shipworm") and by the intense degradation of the organic matter (OM). Other boring organisms, probably worms, are indicated by fecal pellets, confirming the long term drifting hypothesis.

**Acknowledgments:** Thanks are due to the Austrian Science Fund (FWF) for financial support (Project P20018-N10). Sincere thanks go to Evelyn Kustatscher, Benno Baumgarten and Vito Zingerle (all Museum of Nature South Tyrol) for their help in organizational issues. I thank Arthur Kammerer, Astrid Wiedenhofer and Valentin Schroffenegger (all Office for Natural Parks South Tyrol) for working permits in the Puez-Geisler Nature Park. Preparation work on the rock samples and thin sections was done by Anton Englert (Vienna) and Franz Topka (Vienna). Photographs were taken by Alice Schumacher (Vienna).

## References

- Alexander R., Larcher A.V., Kagi R.I. & Price P.L. 1992: An oil-source correlation study using age specific plant-derived aromatic biomarkers. In: Moldowan M.J., Albrecht P. & Philip P.R. (Eds.): Biological markers in sediments and petroleum. *Prentice-Hall, Englewood Cliffs, N.J.*, 201–221.
- Blumenberg M., Krüger M., Nauhaus K., Talbot H.M., Oppermann B.I., Seifert R., Pape T. & Michaelis W. 2006: Biosynthesis of hopanoids by sulfate-reducing bacteria (genus *Desulfovibrio*). *Environ. Microbiol.* 8, 1220–1227.
- Bosellini A., Gianolla P. & Stefani M. 2003: Geology of the Dolomites. *Episodes* 26, 3, 181–185.
- Bray E.E. & Evans E.D. 1961: Distribution of n-paraffins as a clue to recognition of source beds. *Geochim. Cosmochim. Acta* 22, 2–15.
- Caracuel J., Oloriz F. & Sarti C. 1997: Environmental evolution during the Late Jurassic at Lavarone (Trento Plateau, Italy). *Palaeogeogr. Palaeoclimatol. Palaeoecol.* 135, 163–177.
- Castellarin A., Vai G.B. & Cantelli L. 2006: The Alpine evolution of the Southern Alps around the Guidicarie faults: A Late Cretaceous to Early Eocene transfer Zone. *Tectonophysics* 414, 203–223.
- Cecca F. 1998: Early Cretaceous (pre-Aptian) ammonites of the Mediterranean Tethys: palaeoecology and palaeobiography. *Palaeogeogr. Palaeoclimatol. Palaeoecol.* 138, 305–323.
- Cranwell P.A. 1977: Organic geochemistry of CamLoch (Sutherland) sediments. *Chem. Geol.* 20, 205–221.
- Dercourt J., Ricou L.E. & Vrielynck B. (Eds.) 1993: Atlas Tethys Palaeoenvironmental Maps. Explanatory notes. *Gauthier-Villars, Paris*, 1–307 (14 maps, 1 pl.).
- Didyk B.M., Simoneit B.R.T., Brassell S.C. & Eglinton G. 1978: Organic geochemical indicators of paleoenvironmental conditions of sedimentation. *Nature* 272, 216–222.
- Eglinton G. & Hamilton R.J. 1967: Leaf epicuticular waxes. *Science* 156, 1322–1335.
- Fourcade E., Azema J., Cecca F., Dercourt J., Guiraud R., Sandulescu M., Ricou L.-E., Vrielynck B., Cottreau N. & Petzold M. 1993: Late Tithonian (138 to 135 Ma). In: Dercourt J., Ricou L.E. & Vrielynck B. (Eds.): Atlas Tethys Palaeoenvironmental Maps. Explanatory Notes. *Gauthier-Villars, Paris*, 113–134.
- Goossens H., de Leeuw J.W., Schenck P.A. & Brassell S.C. 1984: Tocopherols as likely precursors of pristane in ancient sediments and crude oils. *Nature* 312, 440–442.
- ten Haven H.L., de Leeuw J.W., Rullkötter J. & Sinninghe Damsté J.S. 1987: Restricted utility of the pristane/phytane ratio as a palaeoenvironmental indicator. *Nature* 330, 641–643.
- Jud R. 1994: Biochronology and systematics of Early Cretaceous radiolarian of the Western Tethys. *Mém. Géol.*, Lausanne 19, 1–147.
- Killops S.D. & Killops V.J. 1993: An introduction to organic geochemistry. *Harlow: Longman; copublished in the USA by John Wiley*, xiii+265 pp.
- Laflamme R.E. & Hites R.A. 1978: The global distribution of polycyclic aromatic hydrocarbons in recent sediments. *Geochim. Cosmochim. Acta* 42, 289–303.
- Lukeneder A. 2008: The ecological significance of solitary coral and bivalve epibionts on Lower Cretaceous (Valanginian–Aptian) ammonoids from the Italian Dolomites. *Acta Geol. Pol.* 58, 4, 425–436.
- Lukeneder A. 2010: Lithostratigraphic definition and stratotype for the Puez Formation: formalization of the Lower Cretaceous in the Dolomites (S. Tyrol, Italy). *Austrian J. Earth Sci.* 103, 138–158.
- Lukeneder A. 2011: The Biancone and Rosso Ammonitico facies of the northern Trento Plateau (Dolomites, Southern Alps, Italy). *Ann. Naturhist. Mus. Wien, Ser. A* 113, 9–33.
- Lukeneder A. 2012: New biostratigraphic data of an Upper Hauterivian–Upper Barremian ammonite assemblage from the Dolomites (Southern Alps, Italy). *Cretaceous Research* 35, 1–21.
- Lukeneder A. & Aspmair C. 2006: Stratigraphic implication of a new Lower Cretaceous ammonoid fauna from the Puez area (Valanginian–Aptian, Dolomites, Southern Alps, Italy). *Geo. Alp.* 3, 55–91.
- Mackenzie A.S. & Maxwell J.R. 1981: Assessment of thermal maturation in sedimentary rocks by molecular measurements. In: Brooks J. (Ed.): Organic maturation studies and fossil fuel exploration. *Academic Press, London*, 239–254.
- Mackenzie A.S., Brassell S.C., Eglinton G. & Maxwell J.R. 1982: Chemical fossils: the geological fate of steroids. *Science* 217, 491–504.
- Muttoni G., Erba E., Kent D.V. & Bachtadse V. 2005: Mesozoic Alpine facies deposition as a result of past latitudinal plate motion. *Lett. Nat.* 434, 59–63.
- Noble R.A., Alexander R., Kagi R.I. & Knox J. 1985: Tetracyclic diterpenoid hydrocarbons in some Australian coals, sediments and crude oils. *Geochim. Cosmochim. Acta* 49, 2141–2147.
- Otto A. & Wilde V. 2001: Sesqui-, di-, and triterpenoids as chemosystematic markers in extant conifers — a review. *Bot. Rev.* 67, 141–238.
- Ourrison G., Albrecht P. & Rohmer M. 1979: The hopanoids: palaeo-chemistry and biochemistry of a group of natural products. *Pure Appl. Chem.* 51, 709–729.
- Philip R.P. 1985: Fossil fuel biomarkers. Applications and spectra. *Meth. Geochem. Geophys.* 23, 1–294.
- Préat A., Morano S., Loreau J.-P., Durlet C. & Mamet B. 2006: Petrography and biosedimentology of Rosso Ammonitico Vero-

- nese (middle-upper Jurassic, north-eastern Italy). *Facies* 52, 265–278.
- Radke M., Willsch H. & Welte D.H. 1980: Preparative hydrocarbon group type determination by automated medium pressure liquid chromatography. *Anal. Chem.* 52, 406–411.
- Rohmer M., Bissert P. & Neunlist S. 1992: The hopanoids, prokaryotic triterpenoids and precursors of ubiquitous molecular fossils. In: Moldowan J.M., Albrecht P. & Philp R.P. (Eds.): Biological markers in sediments and petroleum. *Prentice Hall, Englewood Cliffs*, N.J., 1–17.
- Scotese C.R. 2001: Atlas of Earth History. Paleomap project. Arlington, Texas, 1–52.
- Simoneit B.R.T. & Mazurek M.A. 1982: Organic matter of the troposphere. II. Natural background of biogenic lipid matter in aerosols over the rural western United States. *Atmos Environ.* 16, 2139–2159.
- Stampfli G.M., Borel G.D., Marchant R. & Mosar J. 2002: Western Alps geological constraints on western Tethyan reconstructions. In: Rosenbaum G. & Lister G.S. (Eds.): Reconstruction of the evolution of the Alpine-Himalayan Orogen. *J. Virtual Explorer* 8, 77–106.
- Stampfli G. & Mosar J. 1999: The making and becoming of Apulia. *Mém. Sci. Géol. (University of Padova). Spec. Vol., 3<sup>rd</sup> Workshop on Alp. Geol.*, Padova 51, 1.
- Stewart W.N. 1983: Palaeobotany and the evolution of plants. *Cambridge University Press*, Cambridge, 1–348.
- Tappeiner 2003: Naturpark Puez-Geisler. Panoramakarte. Tappeiner, Lana.
- Tissot B.T. & Welte D.H. 1984: Petroleum Formation and occurrences. 2<sup>nd</sup> Edition. *Springer Verlag*, Berlin, 1–699.
- Volkman J.K. 1986: A review of sterol markers for marine and terrigenous organic matter. *Org. Geochem.* 9, 83–99.
- Volkman J.K. & Maxwell J.R. 1986: Acyclic isoprenoids as biological markers. In: Johns R.B. (Ed.): Biological markers in the sedimentary record. *Elsevier*, Amsterdam, 1–42.
- Volkman J.K., Barrett S.M. & Blackburn S.I. 1999: Eustigmatophyte microalgae are potential sources of C<sub>29</sub> sterols, C<sub>22</sub>–C<sub>28</sub> n-alcohols and C<sub>28</sub>–C<sub>32</sub> n-alkyl diols in freshwater environments. *Org. Geochem.* 30, 307–318.
- Welte D.H. & Waples D. 1973: Über die Bevorzugung geradzahligter n-Alkane in Sedimentgesteinen. *Naturw.* 60, 516–517.
- Zharkov M.A., Murdmaa I.O. & Filatova N.I. 1998: Paleogeography of the Berriasian-Barremian Ages of the Early Cretaceous. *Strat. Geol. Corr.* 6, 47–69.